JOURNAL OF GEOPHYSICAL RESEARCH, VOL. 101, NO. B5, PAGES 11,553–11,564, MAY 10, 1996

Resonance and elastic nonlinear phenomena in rock

Paul A. Johnson[1]
Los Alamos National Laboratory, Los Alamos, New Mexico

Bernard Zinszner and Patrick N. J. Rasolofosaon
Institut Français du Pétrole, Rueil Malmaison, France

Abstract. In a great variety of laboratory experiments over large intervals in stress, strain, and frequency, rocks display pronounced nonlinear elastic behavior. Here we describe nonlinear response in rock from resonance experiments. Two important features of nonlinear resonant behavior are a shift in resonant frequency away from the linear resonant frequency as the amplitude of the disturbance is increased and the harmonics in the time signal that accompany this shift. We have conducted Young's mode resonance experiments using bars of a variety of rock types (limestone, sandstone, marble, chalk) and of varying diameters and lengths. Typically, samples with resonant frequencies of approximately 0.5–1.5 kHz display resonant frequency shifts of 10% or more, over strain intervals of 10^{-7} to 10^{-6} and under a variety of saturation conditions and ambient pressure conditions. Correspondingly rich harmonic spectra measured from the time signal progressively develop with increasing drive level. In our experiments to date, the resonant peak is observed to always shift downward (if indeed the peak shifts), indicating a net softening of the modulus with drive level. This observation is in agreement with our pulse mode and static test observations, and those of other researchers. Resonant peak shift is not always observed, even at large drive levels; however, harmonics are always observed even in the absence of peak shift when detected strain levels exceed 10^{-7} or so. This is an unexpected result. Important implications for the classical perturbation model approach to resonance results from this work. Observations imply that stress-strain hysteresis and discrete memory may play an important role in dynamic measurements and should be included in modeling. This work also illustrates that measurement of linear modulus and Q must be undertaken with great caution when using resonance.

Introduction

Observation of nonlinear elastic response in rock is not a new or novel revelation. For example, one well known manifestation of this behavior is demonstrated by countless quasi-static measurements on rock of velocity (or modulus) versus applied stress [e.g., *Birch*, 1966]. These tests show a strong nonlinear dependence between stress and strain (or modulus and stress), in addition to the phenomena of hysteresis and discrete memory (also termed end point memory) [e.g., *Holcomb*, 1981]. These phenomena are due primarily to compliant features in the rock (cracks, grain boundaries, joints, etc.) [e.g., see *Gist*, 1994] and fluid effects. More recent dynamic studies of transient waves in rock at atmospheric pressure demonstrate that rock has a large nonlinear response at relatively small strains [e.g., *Van Den Abeele*, 1996; *Johnson and Rasolofosaon*, 1996; *Guyer et al.*, 1995a, b; *Liu*, 1994; *Johnson and McCall*, 1994; *Meegan et al.*, 1993; *Ostrovsky*, 1991; *Bakulin and Protosenya*, 1982; *Bonner and Wanamaker*, 1991; *Johnson and Shankland*, 1989; *Zinov'yeva et al.*, 1989; *Beresnev and Nikolaev*, 1988; *Johnson et al.*, 1987; *Bulau et al.*, 1984]. The existence of a significant nonlinear elastic response at even moderate strains is not commonly appreciated.

Our intention here is to describe, and in some cases, to interpret manifestations of nonlinear elastic phenomena induced by resonating a bar of rock in Young's mode. We will emphasize resonant peak shift and harmonic generation, but other unexpected, complex behavior resulting from resonant excitation as observed in some rocks such as chalk will also be described. A surprising result of our work is that nonlinear behavior is not necessarily linked with resonant peak shift. That is, resonant peak shift always indicates that the material is responding nonlinearly; however, nonlinear response may exist without measurable resonant peak shift. On the other hand, it will also be shown that resonant peak shift may begin at even the lowest drive levels in rock and that peak shift and peak width is dependent on sweep direction. This result illustrates that measurement of moduli and Q must be undertaken with great caution.

In the first section the classical theoretical approach to describing a nonlinear oscillator will be illustrated. Following this, the experimental procedure will be described, followed by sections describing the results, discussion, and conclusions.

Qualitative Theory and Measured Quantities

Nonlinear resonance has been discussed by many authors and treatments can be found in numerous texts [e.g., *Stoker*, 1950]. It is not our purpose here to review theory in detail. This

[1]Also at Université Pierre et Marie Curie, Laboratoire d'Acoustique Physique, Paris.

Paper number 96JB00647.
0148-0227/96/96JB-00647$09.00

has already been done by *Guyer et al.* [1995a, b], *Van Den Abeele* [1996], and others. Therefore the nonlinear resonance theoretical development will be only briefly covered in this section as it relates to the measurements taken and the quantities calculated.

In the classical approach to describing wave propagation in a nonlinear material, the energy density is expressed as a function of the scalar invarients of the strain tensor [e.g., *Landau and Lifshitz*, 1986]. The strain energy is typically expanded to higher order resulting in an equation of state where stress is expressed as a function of the strain by a series expansion of the modulus in strain. The standard approach applied to one dimensional problems is for a lumped element (spring-mass) system, as discussed by *McCall* [1993], *Guyer et al.* [1995a, b], *Van Den Abeele* [1996], and others. This approach leads to the equation of motion for the displacement field of

$$\frac{\partial^2 u}{\partial t^2} = \frac{\partial}{\partial x}\left(c^2 \frac{\partial u}{\partial x}\right). \tag{1}$$

Here,

$$c^2 = c_0^2\left[1 + \beta\left(\frac{\partial u}{\partial x}\right) + \delta\left(\frac{\partial u}{\partial x}\right)^2 + \cdots\right], \tag{2}$$

c is the perturbed wave speed, c_0 is the unperturbed wave speed, u is the displacement, $\partial u/\partial x$ is strain ε, and β and δ are coefficients that characterize cubic and quartic anharmonicities (they are the nonlinear coefficients). The equation of motion is generally solved by perturbation theory, using $u = u_0 + u_p$ with u_0 being the linear displacement and u_p its perturbation (the method of characteristics is also a commonly applied approach [e.g., *Courant and Friedrichs*, 1948]). If u_0 is an initially periodic function, for example $[A \cos(\omega_0\tau)]$, where $\tau = t - x/c_0$, the equation of motion will contain terms such as $[A^2 \sin^2(\omega_0\tau)]$ and $[A^3 \sin^3(\omega_0\tau)]$. Trigonometric expansion shows that other frequencies such as $\cos(2\omega_0\tau)$ and $\cos(3\omega_0\tau)$, etc., are created. This is fundamentally the classical explanation for the existence of harmonics. Without the higher-order strain dependent terms in velocity, harmonics do not exist: the system is linear.

In the classical treatment of resonance, the bar is treated as a lumped element responding to

$$\partial u^2/\partial t = -k^2 c^2 u, \tag{3}$$

where k is wavenumber and c is the wave speed shown in (2). The average of the strain field over one period is assumed zero (it may not be), so the quadratic term β is normally eliminated. Therefore, using classical theory, it is the determination of δ that is the goal of the resonance experiment. Following *Guyer et al.* [1995b], the term proportional to δ can be replaced by its time-averaged value:

$$\delta\langle\varepsilon^2\rangle_t = \delta|(\partial u/\partial x)^2| \approx \delta(\varepsilon_M)^2, \tag{4}$$

in which ε_M is the maximum strain magnitude along the bar. Equation (2) can then be rewritten as

$$\frac{c^2 - c_0^2}{c_0^2} \approx \frac{\omega^2 - \omega_0^2}{\omega_0^2} \approx 2\left[\frac{\omega - \omega_0}{\omega_0}\right] \approx 2\left[\frac{\Delta\omega}{\omega_0}\right] \approx \delta(\varepsilon_M)^2, \tag{5}$$

where ω_0 is the angular frequency of the "linear" resonant peak and ω is the angular frequency of the resonant peak as it shifts with strain amplitude. Our experiments are configured to measure Q, ω, and ω_0 and the acceleration $(\partial^2 u/\partial t^2)$ at any desired drive level or frequency, at the opposite end of the bar that is driven. Therefore we can, in applying classical theory, determine δ, the cubic nonlinear parameter.

We are also capable of measuring the harmonic amplitudes of the time signal, typically when the resonance is at maximum value, using the identical experimental configuration. Using a wave propagation result as a comparison, we can obtain a δ from measurement of the third harmonic amplitude:

$$\delta \approx -\frac{(\partial^2 u_3/\partial t^2)\omega_0^4 L^2}{(\partial^2 u_1/\partial t^2)^3}, \tag{6}$$

where L is the bar length, $(\partial^2 u_3/\partial t^2)$ is the acceleration of the third harmonic at resonance, and $(\partial^2 u_1/\partial t^2)$ is the acceleration of the fundamental frequency at resonance. Similarly, from the second harmonic amplitude (if it exists) we can obtain an approximation of β:

$$\beta \approx -\frac{(\partial^2 u_2/\partial t^2)\omega_0^2 L}{(\partial^2 u_1/\partial t^2)^2}. \tag{7}$$

A classical result from analysis of nonlinear oscillators [e.g., *Stoker*, 1950] is that they are hysteretic in their amplitude-frequency behavior (not to be confused with hysteresis in stress versus strain!). That is, the measured acceleration (likewise strain and displacement) depends on which direction the driving frequency is swept, meaning that the amplitude is not uniquely determined by the applied forcing function. This behavior will be illustrated in the results section.

The lumped element assumption implies that stress σ, strain ε, and displacement u are homogeneous in the sample as a function of time. In reality, this is not the case because the system is elastic. Stress and strain are maximum at the center of the bar (in absolute value) and minimum at the bar ends. Displacement is maximum at the bar ends and minimum in the bar center; however, solution to the elastic resonance equation of motion provides nearly identical results to those above.

We are interested in the frequency response as a function of strain, in general, because this is a standard quantity in geophysics. What is actually measured is time-averaged acceleration,

$$\langle\ddot{u}\rangle_t = \left\langle\frac{\partial^2 u}{\partial t^2}\right\rangle_t \approx \omega_0^2\langle u\rangle_t = \omega_0^2 A. \tag{8}$$

Because the first longitudinal resonance mode occurs when the wavelength is precisely half the bar length, the strain is

$$\varepsilon = \frac{\partial u}{\partial x} \approx \frac{-i\omega_0}{c_0}u = -i\frac{2}{L_0}u, \tag{9}$$

where again u is displacement and L_0 is the bar length at rest. From (8) and (9) the maximum strain magnitude is then

$$\varepsilon_M = \langle\varepsilon\rangle_t = 2\frac{\langle\ddot{u}\rangle_t}{L_0\omega^2}. \tag{10}$$

The displacement amplitude at the bar ends is given by $\langle\ddot{u}\rangle_t/\omega_0^2$.

Linear Young's modulus E_0, another quantity that will be illustrated, is obtained from the fundamental resonance frequency measured at low drive voltage in the strain interval of 10^{-8}–10^{-9} (approximately linear regime). From the mass density ρ and length L the modulus is

$$E_0 = \rho_0 C_E^2 = \rho_0 \frac{L_0^2 \omega_0^2}{\pi^2} \quad (11)$$

where ω_0 is the fundamental resonant bar frequency at linear elastic strain and C_E is the Young's mode velocity at ω_0.

Experimental Procedure

The basic elements of the experimental configuration for obtaining frequency versus acceleration measurements are shown in Figure 1. We use both an analog or digital experimental apparatus, depending on the desired result. In general, the analog method is superior when it is necessary to observe a large dynamic range. The digital method is fast and convenient but has the disadvantage of a smaller dynamic range.

Using the analog method, a frequency sweep interval that is chosen to encompass frequencies well above and well below the fundamental resonant mode of the sample is used. The signal is amplified and acoustically excited by an electromagnetic (coil/magnet) source affixed parallel to the axis of the sample. Piezoelectric and shaker-type sources are also used. The signal is detected by use of a calibrated accelerometer, time averaged, and frequency versus maximum acceleration is plotted and/or stored digitally. A digital oscilloscope is used for monitoring the time series signal. Measurements are made of both upward and downward frequency sweeps over the chosen interval. Typically, 5–20 experiments are conducted at successively increasing drive voltages over the same frequency interval in order to monitor resonant peak shift and harmonic generation. A single sweep is typically 1–5 min in duration, depending on the Q of the material. For accurate results, high-Q materials tend to require a longer sweep time.

The digital measurements are made with a PC that contains a card that has both a function generator and a heterodyne detector. In this configuration, a constant amplitude drive signal output from the card is multiplied with the detected signal from the rock. The multiplied signal is time averaged and low-pass filtered providing a dc output proportional to the detected acceleration. The PC also contains a 16-bit A-D card for capturing time signals for harmonic analysis.

Measurements of at least nine different rock samples were made. These include Berea sandstone [see, e.g., *Krech et al.*, 1974], Meule sandstone, Lavoux limestone, magnesium marble, Estaillades limestone, St. Pantaleon limestone, Asian marble, Chalk, Fontainebleau sandstone, and Carrera marble (for more information regarding these rocks, excluding the Berea, see *Lucet and Zinszner* [1992]). Comparative studies were conducted using the relatively elastically linear materials aluminum, PVC, Plexiglas, Pyrex glass, porous sintered aluminum, and polycarbonate. For several rock samples, including Meule sandstone, Lavoux limestone, and chalk, measurements were taken at numerous water saturation levels between approximately 1 and 99%. In each case, the sample was saturated after evacuation, and measurements were made as the rock dried under room conditions. Densities were estimated from the dry weight and the measured porosity. Sample lengths ranged from 0.30 to 1.15 m and diameters ranged from 0.025 to 0.105 m.

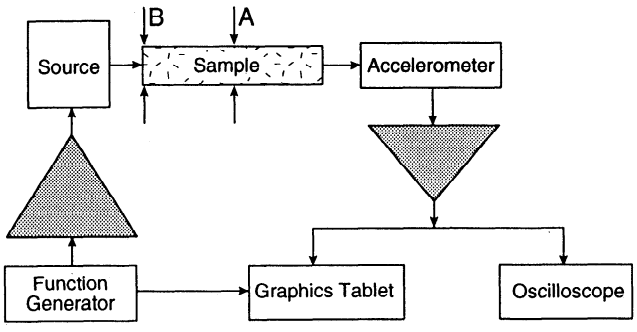

Figure 1. Experimental configuration. A and B refer to locations of pulse mode travel time measurements. See text for further explanation.

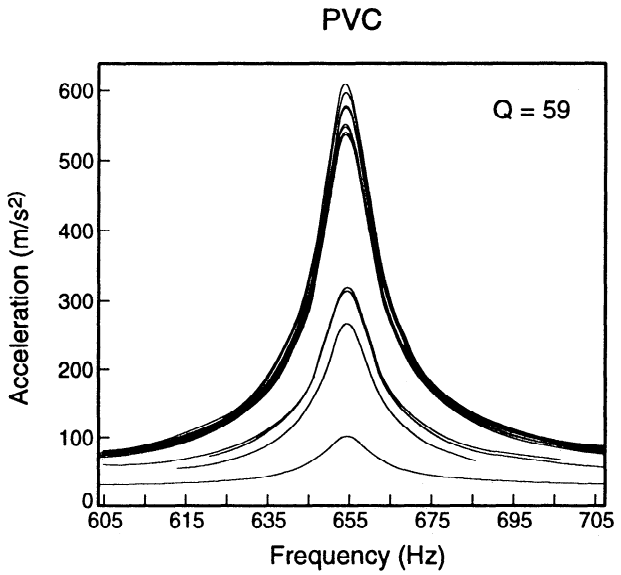

Figure 2a. Detected acceleration versus swept frequency for a sequence of resonance curves at twelve different excitation levels in polyvinyl chloride (PVC). Both downward and upward frequency sweeps are plotted; however, they are indistinguishable from each other (Note that the wobbly character of the curves is due entirely to the digitizing process for graphics representation and has nothing to do with the material characteristics.)

Results

Typical Behavior of Elastically "Linear" Solids

Figure 2a shows a sample sequence of resonance curves for twelve different excitation levels in polyvinyl chloride (PVC), a material that is relatively elastically "linear" in comparison with most rocks. Figure 2a shows detected acceleration versus swept frequency. Both downward and upward frequency sweeps were conducted at each drive level; however, they are indistinguishable from each other. Note the Q (59) is similar to many rocks. Figure 2b shows excitation-strain data collected at the resonant peak excitations in polycarbonate, another "linear" material, from a nearly identical experiment to that shown in Figure 2a (the resonant peaks are of the same character as those for PVC, i.e., no peak shift is observed). Note that the excitation versus strain curve is related to stress versus strain because excitation is linearly proportional to stress. The experiment differs slightly in that at each resonant peak, the drive frequency and excitation level are held constant, while the time signal is collected and averaged to improve the signal to noise ratio. The averaged signal is then Fourier analyzed, and the

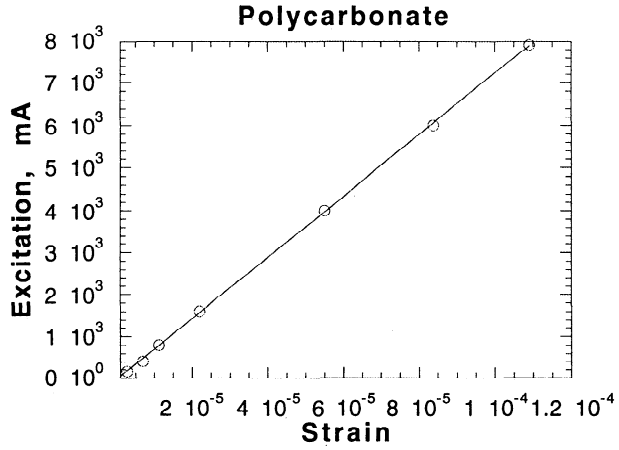

Figure 2b. Excitation level versus strain in polycarbonate, another "linear" material compared to rock. The solid line shows the fit to the data (open circles) of the drive excitation level in milliamperes (Y axis) versus the strain level (X axis). Error bars are of the order of the circle sizes. The harmonic ratio, if it existed over this strain interval, would be plotted as well; as there were no harmonics observed, none are plotted. Note that the resonance curves show no peak shift, just as those for PVC.

relative harmonic amplitudes are measured. In this strain range, no harmonics were observed. In addition, all of the "linear" materials studied have a constant derivative of ∂(excitation)/$\partial\sigma$, that is, a linear stress-strain relation, implying they have a single modulus in the strain ranges studied (see below). This plot will be compared to that for a rock shortly.

We indicate several key observations from Figures 2a and 2b that can be regarded as representative for "linear" solids. In general, these materials: (1) show no detectable peak shift; (2) display a linear relationship between excitation and strain; and (3) show a low level of harmonics compared to rock.

Based on the resolution of our system we consider that the level of harmonic generation in "linear" solids is near the limit of our current resolution (using a 12-bit digital oscilloscope and averaging signals). These three observations are representative of all of the "linear" elastic materials listed above (as cautionary note, the experimental apparatus does not provide the frequency resolution to quantitatively study high-Q materials such as aluminum). When harmonics are observed in these materials, they are inferred to originate from the response of the materials themselves because harmonics are not observed in all of the "linear" elastic materials (e.g., sintered aluminum), and the relative harmonic levels vary from "linear" material to material. This would not be the case if the source (especially electromagnetic hysteresis) or electronics were the cause or the harmonics. The results of attenuation, sample dimensions, frequency shift, modulus, detection of harmonics, and strain levels on elastically "linear" materials studied are displayed in Table 1. The values for attenuation were obtained after careful inspection of the data to be certain that the results were not influenced by the existence of harmonics and peak shift.

Typical Behavior of Elastically Nonlinear Solids: Rock

In Figure 3a, a representative result for Young's mode resonant behavior in rock is shown. The material is Lavoux limestone under ambient conditions. Compare this result to that of PVC shown in Figure 2a. The difference in the character of the resonance sweeps as a function of amplitude is striking. Figure 3b shows results for Fontainebleau sandstone also at ambient conditions. The middle plot of Figure 3b shows the resonant peak shift, and the bottom and top plots show the corresponding time and frequency domain signals at low (but nonlinear) drive level and large drive level, respectively. Note that the linear resonant response has been expanded vertically in both Figures 3a and 3b in the insets.

Peak Shift and Frequency Hysteresis in Rock

In the resonance sweeps shown in Figures 3a and 3b, the solid lines represent downward frequency sweeps, and the dashed lines represent upward frequency sweeps. Two observations are of note. First, the peak shift is marked as a function of detected acceleration in these samples. Second, the shape of the curve depends on in which direction the sweep takes place, upward or downward in frequency. This second observation is typical of nonlinear oscillators in general [e.g., see *Stoker*, 1950]. Qualitatively, the resonant frequency shift and the dif-

Table 1. Coefficients for Elastically "Linear" Materials

Material	Q	Length × Diameter, cm	Slope of Frequency Shift (Equation (5))	Excitation-Strain Derivative	Harmonics Detected	Maximum Detected Strain
Sintered aluminum	290	100. × 8.	UD	linear	none	1.2×10^{-5}
Plexiglas	27	34. × 4.	UD	linear	2, 3, 4	4.4×10^{-6}
PVCa	59	120. × 8.	UD	linear	2,	3.0×10^{-6}
PVCb	59	61.2 × 10.5	UD	linear	2, 4, 3, 6, 5 ,7	5.3×10^{-6}
Aluminum	>50,000	35. × 4.	UD	linear	2, 3, 4	2.2×10^{-5}
Pyrex glass	2750	93.8 × 4.	UD	linear	2	2.2×10^{-5}
Polycarbonate	130	101.6 × 4.	UD	linear	2, 3, 4	1.1×10^{-4}

Data shown are inverse attenuation Q; sample length and diameters; the slope of the frequency shift from equation (5) which theoretically provides a measure of δ; the derivative of the excitation versus strain plot which is directly related to the modulus (it is only indicated whether or not the slope is linear, i.e., constant modulus and a linear equation of state); whether or not harmonics were detected in the time signal at resonance; and maximum detected strain levels. The numbers of the harmonics show which harmonics were detected and the relative dominance in amplitude of observed harmonic amplitudes over the range of strain observation. For example, aluminum shows that the second, fourth, and fifth harmonics were observed, and each successive harmonic amplitude over the range measured was relatively smaller in amplitude. On the other hand, PVCb shows that the fourth harmonic amplitude dominated over the third, etc. The PVC samples only differed in dimension. UD (undetectable) indicates that there was no detectable frequency shift using our apparatus.

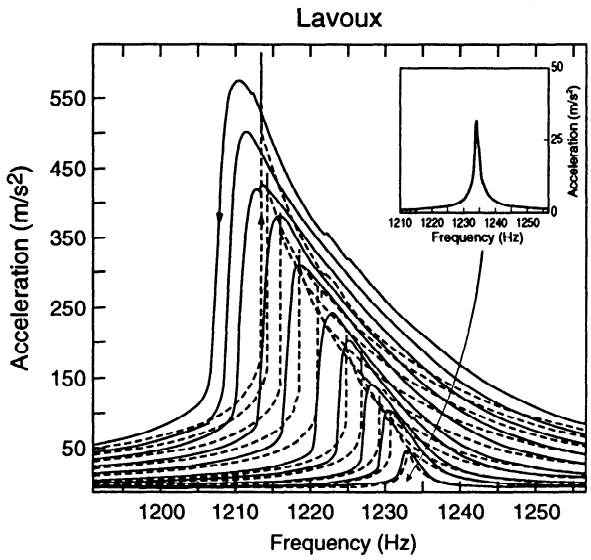

Figure 3a. Elastic nonlinear behavior in a rock. Acceleration versus frequency for nine excitation levels in Lavoux sandstone at ambient conditions. The inset shows the character of the linear behavior at an expanded scale.

ference in upward and downward resonant behavior (frequency hysteresis) can be thought of as follows. Initially, the modulus is in its at rest (clastically "linear") state. At very low, but successively increasing drive levels, the resonant response may (but not always) remain at the same frequency, as has been shown by others [e.g., *Winkler et al.*, 1979; *Murphy*, 1982; *Bulau et al.*, 1984]. As the source drive level is increased, the material net modulus begins to drop, and this is reflected in a drop in the resonant frequency. As the drive frequency approaches the modified resonant frequency, naturally, the excitation becomes larger as well. Larger excitation induces the net modulus to drop even further, and the resonant frequency in effect "chases" the resonant peak as it steadily shifts downward in response to larger and larger excitation. This cause and effect relationship takes place until the bar reaches some maximum energy state proportional to the maximum input energy in the sample. At this point, as the frequency is decreased further, it passes through the modified resonant peak and the amplitude drops rapidly back to the nonresonant value. The net modulus, and therefore resonance frequency, shifts back to its original, elastically "linear" value. The shift back can be readily observed by conducting a low-amplitude frequency sweep immediately after a high-amplitude sweep.

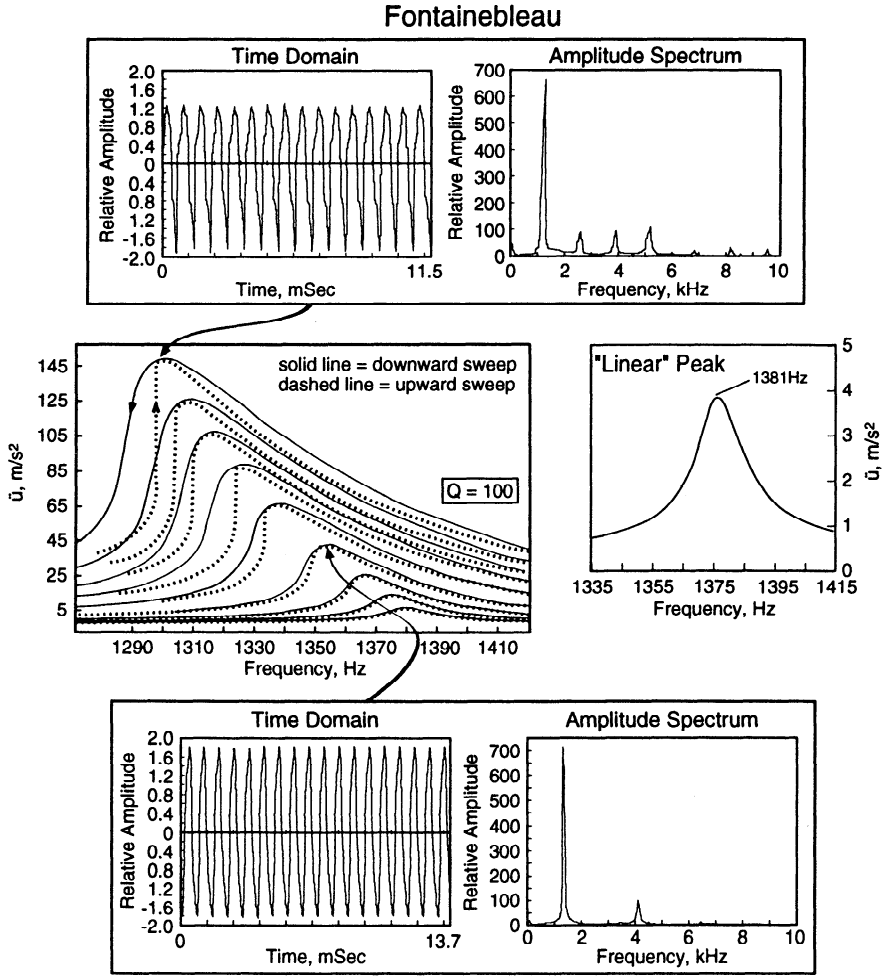

Figure 3b. Acceleration versus frequency for nine excitation levels in Fontainebleau sandstone at ambient conditions. (middle) The resonant peak shift for both upward (dashed lines) and downward (solid lines) frequency sweeps. (bottom) and (top) The corresponding time and frequency domain signals at low (but elastically nonlinear) drive level and large drive level, respectively. The insets shows the character of the linear behavior.

As frequency is swept in the upward direction, the modulus begins again at its rest (elastically linear) state. At larger excitation levels, as the frequency approaches the linear resonant value and more energy is introduced into the resonating bar, the net modulus begins to drop as before. In effect, the maximum energy state (depending on drive level and material property) where the resonant frequency is at minimum (as is the modulus) and the upward swept frequency "meet" and the frequency passes through the modified resonant peak. This process takes place over a very short frequency interval as can be seen by the abrupt increase in acceleration response in Figure 3a. As frequency increases further, the resonant peak is modified upward but lags behind the sweep frequency in the experiments shown. As before, the modulus returns to its at rest state after excitation.

The corresponding time and frequency domain plots (Figure 3b, bottom and top), for two different resonance peaks corresponding to two different excitation levels, show typical results. In this case, at low drive (but in the nonlinear response regime), the time signal is distorted, being composed of the fundamental and third harmonic. As the drive level is increased, the time signal becomes highly distorted, is asymmetric, and has a dc component, all manifestations of elastic nonlinear behavior in the material. The corresponding spectrum illustrates the rich spectrum associated with large excitation level. In general, odd harmonics tend to dominate in amplitude in rock, in contrast to the elastically "linear" materials studied above.

Figure 4 shows excitation and harmonic ratio versus strain for the Lavoux Limestone sample at 0.5% water saturation (note the normalization of the quantities, see Figure 4 caption). In this case, only the second and third harmonics were plotted although higher harmonics were present. The plot indicates the following: for dry Lavoux limestone, the third harmonic dominates in amplitude over the second harmonic, and the resonant peak shift commences at a slightly larger strain than the emergence of harmonics. Both the growth of harmonics and the excitation versus strain curve are reasonably representative of dry rocks.

We indicate three fundamental observations from Figures 3 and 4 that can be regarded as representative for rock. These materials (1) generally but not always show resonant peak shift as a function of drive level; (2) generally but not always display a nonlinear relationship between excitation and strain over the strain intervals studied; and (3) can display a rich spectrum of harmonics at strain levels as low as 10^{-7}.

A final observation in regards to resonant peak shift is noteworthy. Depending on the rock and the saturation state, the resonant peak may begin shifting immediately, even at the lowest possible applied drive levels and at strain levels that are extremely small ($<10^{-8}$). This behavior is not an exceptional observation in the rocks that were studied. For example, Berea sandstone shows this behavior at ambient conditions. The onset of peak bending at such small strains is an important consideration for measurement of Q and velocity when applying the resonant bar method.

Change in Resonant Frequency, Harmonics, and Nonlinear Modulus

As indicated from the classical approximation shown in equation (5), the cubic nonlinear parameter δ is obtained from the change in angular resonant frequency ω as a function of the strain ε. Comparison can be made with δ obtained from measurement of the third harmonic amplitude (equation (6)). The quadratic nonlinear parameter β can be obtained from the second harmonic amplitude (equation (7)).

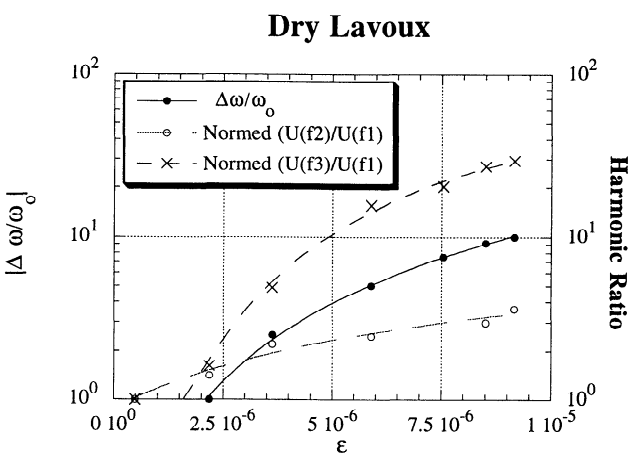

Figure 4. Excitation level versus strain and harmonic ratio versus strain in Lavoux limestone at 0.5% water saturation. The solid line shows the drive excitation level in milliamperes (left-hand Y axis) versus the strain level (X axis). The harmonic ratio of each successive harmonic to the fundamental detected level is shown by the dashed lines. The curves associated with all of the data are second-order polynomial fits shown to aid visualization of the data. The ratio values are shown on the right-hand Y axis, again versus strain. Both $\Delta\omega/\omega_0$ and the harmonic ratios have been normalized to their minimum values. The ratios of the second U(f2), and third U(f3) harmonics relative to the first harmonic U(f1) minimum (the fundamental) are plotted, (U*fi*/Uf1)/(U*fi*/Uf1) at a strain of 4.9148×10^7, where *fi* is f2 or f3. Both f2 and f3 appear first at this strain level in this case. It is clear from the plot that harmonics are observed at a slightly lower strain level than the onset of peak shift. In this case, only the second and third harmonics were measured although higher harmonics were present. Compare to Figure 2b for polycarbonate where no harmonics were observed over this strain interval. Measurement errors are of the same order as the symbol sizes.

We plot $\Delta\omega/\omega_0$ versus strain ε for several data sets. Meule sandstone, Lavoux limestone, St. Pantaleon limestone, Fontainebleau sandstone, and chalk are shown at various saturation conditions in Figure 5. Two observations from Figure 5 are of note: (1) $\Delta\omega/\omega_0$ does not go as the ε^2 as predicted by equation (5); instead, it ranges from a power law relation of approximately 1.0 to 1.5; and (2) at larger strain the slope of $\Delta\omega/\omega_0$ versus ε tends to decrease. The error bars are very small at large $\Delta\omega/\omega_0$ (approximately the diameter of the symbols); however, error bars are larger at small $\Delta\omega/\omega_0$ (up to a factor of 2). Despite this, it is convincing from the large number of data that the slope is not two as predicted by classical theory. This important observation implies the classical theory is inadequate for obtaining the nonlinear modulus from the resonant peak shift in its current state of development for the rocks described in this paper.

Figure 6 shows how the cubic nonlinear parameter is estimated for Berea sandstone, based on the harmonic calculation from equation (6). A similar plot can be made using the second harmonic data using equation (7) to obtain the quadratic parameter. The outstanding result from Figure 6 is that the cubic parameter is far too large ($>|10^{15}|$), based on our, and others, measurements of the cubic parameter from pulse mode and

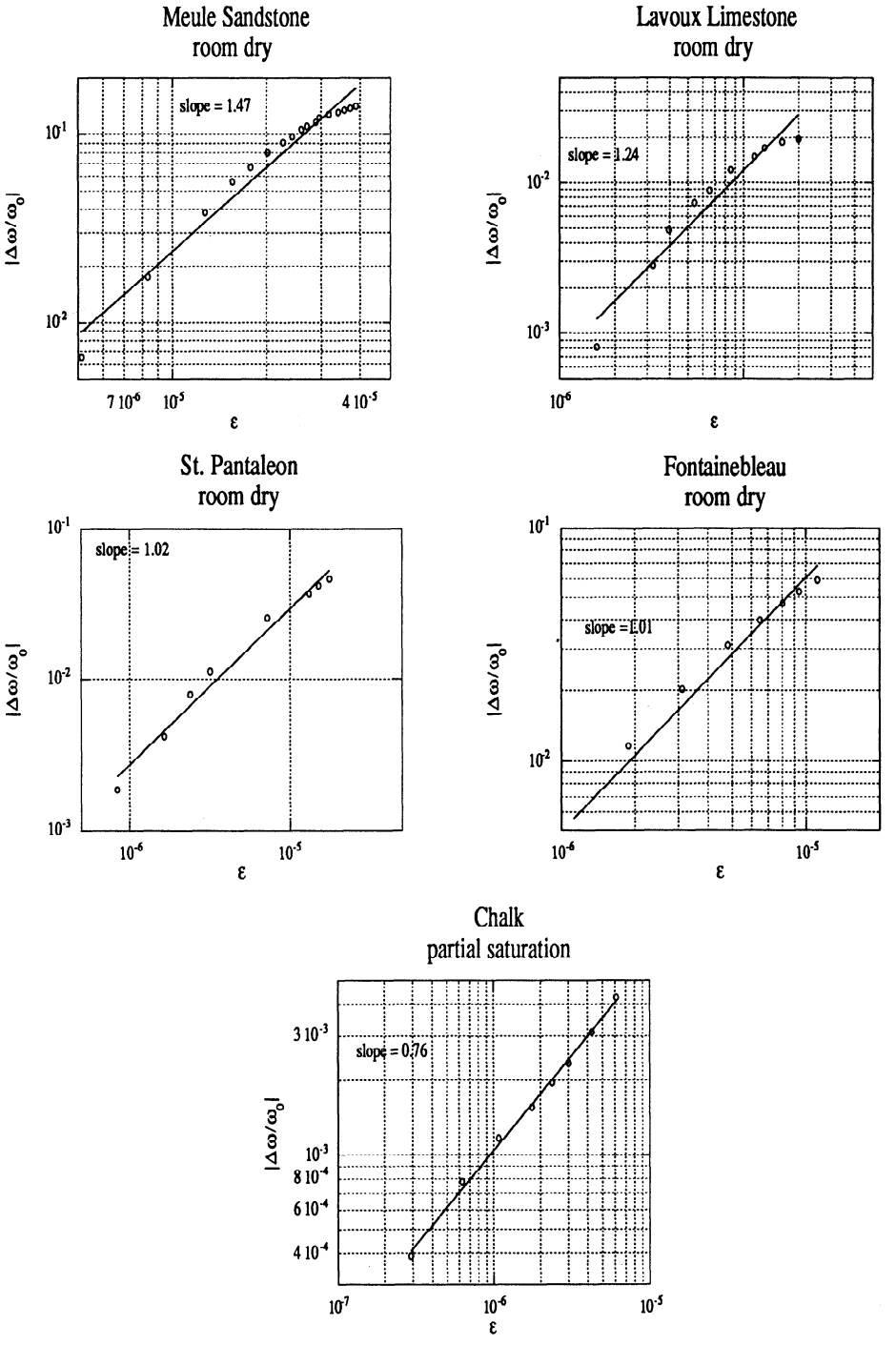

Figure 5. $|\Delta\omega/\omega_0|$ versus strain ε (see equation (5)) for several rocks under various saturation conditions.

static tests. Based on a large number of static tests obtained from the literature, δ should be order 10^6 $\pm$1–2 orders of magnitude (ignoring frequency dependence).

Results for various rocks are tabulated in Table 2 along with their saturation states and Q and δ. Tables 2 and 3 show that δ obtained from the third harmonic and the slope of the frequency shift (δ from the resonant peak shift) is also far larger than expected. The result is the same for the four rocks studied at all saturation states as well. For example, Table 3 shows the results for Lavoux limestone at all saturation states. We will address the above issue further in the discussion section.

Ultrasonic Pulse Mode Velocity Change With Excitation Level

It is an interesting exercise to measure the pulse mode velocity as a function of the resonant excitation and strain level in rock, because we expect the velocity to change. The velocity should decrease with resonance excitation because the net

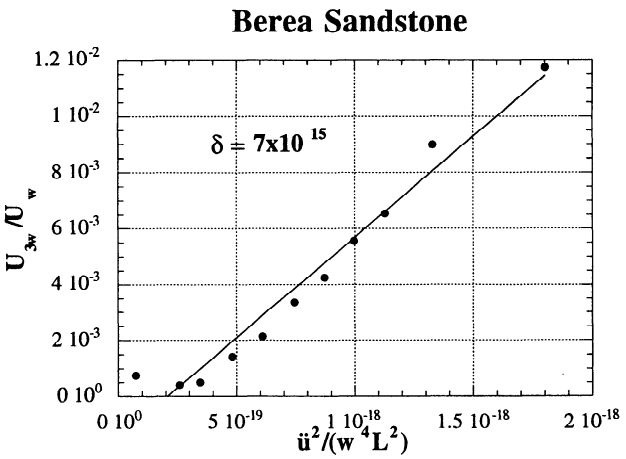

Figure 6. The cubic nonlinear parameter δ obtained from the third harmonic data for Berea sandstone. Measurement errors are of the same order as the symbol sizes; the fit to δ is plus or minus an order of magnitude.

Table 3. Physical Properties as a Function of Saturation in Lavoux Limestone

Q	S_W, %	Slope Frequency Shift	$\lvert\delta\rvert$ (Harmonic)
1000	0.1	-7.36×10^{8}	-1.92×10^{9}
820	0.5	-1.11×10^{9}	-3.59×10^{9}
770	1.0	-1.26×10^{9}	-1.99×10^{9}
700	1.5	-1.60×10^{9}	-9.10×10^{9}
420	4.0	-1.11×10^{9}	-8.07×10^{9}
440	5.0	-6.05×10^{9}	-1.72×10^{9}
440	8.0	-4.62×10^{9}	-3.13×10^{9}
330	20.0	-1.42×10^{10}	-1.45×10^{10}
360	24.0	-9.15×10^{9}	-8.13×10^{9}
350	31.0	-1.39×10^{10}	-1.21×10^{10}
280	45.0	-1.13×10^{10}	-9.15×10^{9}
300	50.0	-9.26×10^{9}	-1.32×10^{10}
310	64.0	-2.04×10^{10}	-7.01×10^{9}
150	73.0	-1.41×10^{10}	-6.24×10^{9}
80	84.0	-1.31×10^{10}	-4.49×10^{10}
45	98.0	-2.51×10^{11}	-9.56×10^{9}

Q was obtained at excitation levels that were linear (no harmonics were observed, and the resonant frequency was stable).

modulus drops as a function of increasing resonance excitation. In this experiment we placed piezoelectric transducers on the top and bottom of the bar near the bar midpoint for lateral measurement of time delay, perpendicular to the axis of resonance excitation (see A in Figure 1). We then conducted the resonant sweep measurements at steadily increasing drive levels as before. When the bar is at peak resonance for each successive excitation level, the time for a pulse to travel across the bar is measured. The experiment was duplicated with transducers very near one end of the bar (B in Figure 1). The two data sets were collected intentionally where the average stress is maximum (bar center) and minimum (bar end). We would expect to see a larger effect where the average stress is largest, if at all (note that the normalized lateral modulus is related to the longitudinal modulus by Poisson's ratio, a nonlinear quantity also).

The results are shown in Figure 7. In each case, the waveform was averaged while the bar resonated over many cycles. Thus an average time delay, or equivalently modulus, was measured across the bar. Errors in measurements are much smaller than the overall change. As expected, there was no measurable change in modulus from near the bar end as shown by the squares. At the bar center, the modulus decreases as a function of excitation level as shown by the dots. This observation is consistent with all results we are aware on rock in that it demonstrates a softening nonlinearity of the rock. The β calculated from the change in modulus is approximately 10^4, a value compatible with β calculated from static measurements.

Complex Nonlinear Elastic Behavior: Chalk

In our investigation we have discovered some additional and unexpected results that seem to be related to rock composition. Chalk is an example of a rock that shows unique behavior relative to the other rocks investigated. An illustration of a sample resonance curve for chalk at a water saturation of about 45% is shown in Figure 8a. Only the "linear" resonance peak (expanded vertical scale in inset) and one high drive level sweep, both upward and downward, are shown. There are two observations that can be made from this plot and from our general experience with chalk.

1. The curves do not resemble those of other rocks; in fact, the curves are an approximate mirror image of the typical behavior in rock. The abrupt transition in amplitude occurs on

Table 2. Physical Properties of Various Rocks, Shift of the Slope ($\lvert\Delta\omega/\omega_0\rvert$ Versus ε^2), Derivative of the Excitation-Strain Curve, and Maximum Detected Strain at the Peak in Resonance

Material	Q	S_W, %	Length × Diameter, cm	Slope of Frequency Shift (Equation (8))	$\lvert\delta\rvert$ (Harmonic)	Excitation-Strain Derivative	Maximum Detected Strain
Estaillades limestone	86	30	116.0 × 8.0	-1.3×10^{10}	3.28×10^{10}	NL	8.8 × 10-7
St. Pantaleon limestone	140	42	115.0 × 8.0	-3.4×10^{10}		NL	1.1 × 10-6
St. Pantaleon limestone	170	18	115.0 × 8.0	-1.3×10^{10}		NL	1.3 × 10-6
ASI marble	360	~0	49.0 × 4.0	-3.1×10^{9}	2.91×10^{9}	NL	3.1 × 10-6
Chalk	225	~0	63.8 × 9.0	-8.4×10^{10}	3.45×10^{14}	NL	1.3 × 10-5
Meule	4.6	98	107.6 × 5.0	-3.8×10^{9}		linear	1.7 × 10-5
Berea sandstone	70	UK	30.1 × 5.0	-4.1×10^{10}		NL	1.4 × 10-6
Fontainebleau sandstone	100	~0	39.0 × 4.0			NL	1.1 × 10-5

Q was obtained at excitation levels that were linear (no harmonics were observed, and the resonant frequency was stable). S_W refers to saturation. ASI, Asian marble; UK, unknown conditions; NL, nonlinear.

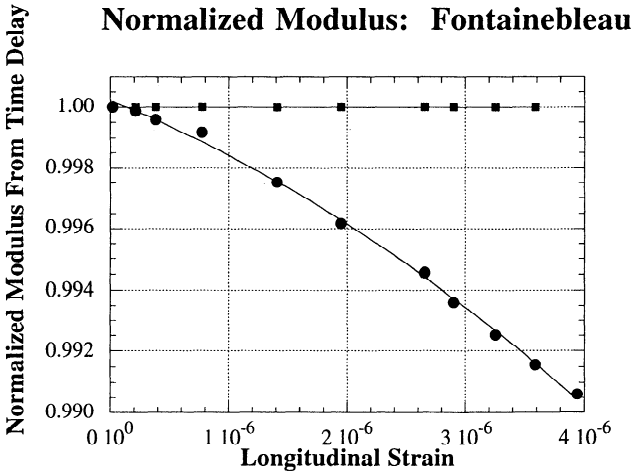

Figure 7. Modulus calculated from time delay across the short direction of a sample of Fontainebleau sandstone during a typical sequence of resonance sweeps. Measurements were made near the bar center (squares) and at near the bar end (dots). The lines are polynomial fits to the data. The result shown was taken at the bar center; that at the bar end shows no change within our precision. Error bars are approximately 2–3 times the size of one dot.

the high-frequency side of the nonlinear resonance curve (compare the plot for Lavoux sandstone in Figure 3a).

2. At large drive level during the downward sweep, the detected signal response oscillates rapidly up and down as it approaches the resonance peak. We made absolutely certain that this was an intrinsic effect to the rock and not related to the electronics, source, or bonding problems.

The harmonic spectrum which was observed but not collected near the region of instability was enormously rich. Harmonics were observed out to at least 50 kHz. Figure 8b shows the excitation level versus strain versus harmonic ratios. Note again the nonlinear excitation-strain curve. Figure 8c shows a plot of the harmonic spectrum for an experiment with dry

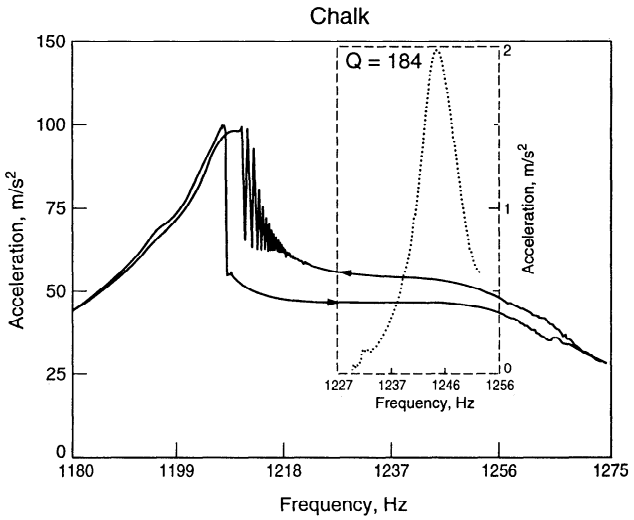

Figure 8a. Resonant sweep data for both upward and downward sweep intervals for partially saturated chalk. Only a low drive and high drive level result are shown. The "linear" peak is not to scale but has been expanded vertically in the inset.

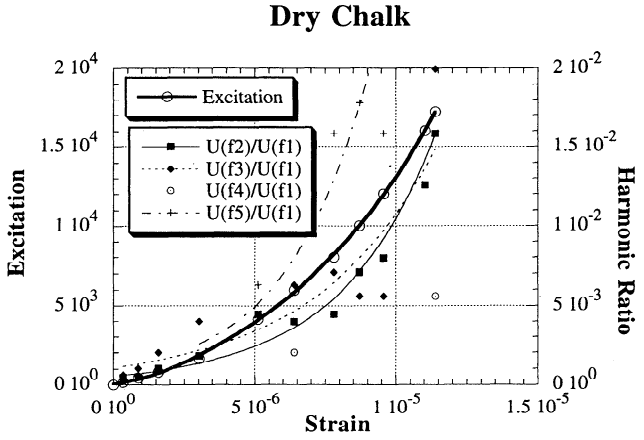

Figure 8b. Excitation-strain-harmonic ratio data for dry chalk. Measurement errors are of the same order as the symbol sizes for the excitation and f1, f3, and f5 harmonics. For f2 and f4 the measurement errors are 2–3 $\times$ 10^{-3} in units of harmonic ratio.

chalk. The plot shows $\Delta\omega/\omega_0$ versus strain versus normalized harmonic ratio for a sample at 0.5% water saturation. The result shown is typical for a dry sample. Interestingly, in contrast to the partially saturated chalk, there is unmeasureable resonant peak shift, as illustrated by the open circles; however, the harmonic spectrum is nonetheless extremely rich. Compare Figure 4 for dry Lavoux limestone. Peak shift and harmonic generation both occur in the Lavoux which is typical of a rock, whereas peak shift is negligible in the chalk, while the harmonic spectrum is rich.

The oscillation in the response for partially saturated chalk shows an instability not obviously present in other rocks. We can only infer that chalk has perhaps the most nonlinear response of any rock we have investigated as demonstrated by the harmonic content. The instability may be indicative of the

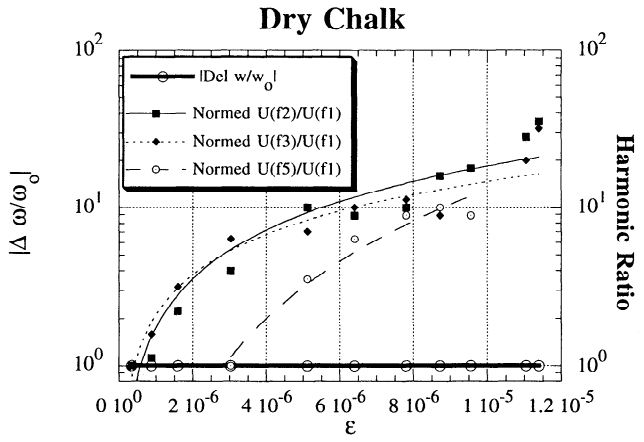

Figure 8c. $\Delta\omega/\omega_0$ versus strain versus harmonic ratio data for dry chalk (slightly different saturation than in Figures 8a and 8b). In this plot, measurement errors are of the same order as the symbol sizes. Both $\Delta\omega/\omega_0$ and the harmonic ratios have been normalized to their minimum values. Note the harmonic generation but unobservable peak shift. In this case, f1 and f2 appear at a strain of 3.4 $\times$ 10^{-7}, whereas f5 appears at a strain of 3.0 $\times$ 10^{-6}. In both Figures 8b and 8c the lines represent polynomial fits to the data to aid the eye.

onset of chaotic behavior. We were unable to collect spectra in this region of instability so this hypothesis is currently not verified. In addition, we can infer from the results for chalk that much of the energy at the fundamental resonance is transferred to harmonics, far more so than in other materials studied. The unique response of chalk is surely due to its unique composition. We are currently conducting detailed studies of chalk.

An important lesson from the chalk is that nonlinearity is not necessarily indicated by peak shift but by monitoring harmonics and that saturation plays an important role in the response of the material. This is a clue to our later discussion on why the classical perturbation theory alone is not suitable for rocks.

Discussion

We believe the nonlinear coefficients derived from a classical perturbation expansion of the resonance wave equation are not realistic in comparison to those obtained from static experiments. We calculate a quadratic nonlinear parameter β of order -10^3 to -10^4 and cubic parameters δ of -10^6 to -10^8 from a diverse suite of data available in the literature for many rock types. Other clues indicating that a model invoking a classical perturbation expansion of the equation of state (or the strain energy function) is incomplete come from some of the results presented in this work. For example, the observation in chalk of a rich harmonic spectrum in the presence of little or no peak shift is one indication. The incorrect power law dependence as predicted by equation (5) and shown by the plots in Figure 5 provides an additional and closely related clue. Evidence from elsewhere suggesting that a classical perturbation expansion is insufficient comes from the large body of published results showing that hysteresis and discrete memory seem to be representative of rock [see, e.g., *Guyer et al.*, 1995a, b; *Boitnott*, 1993; *Holcomb*, 1981].

What are the implications of the existence of hysteresis and discrete memory in a resonating or propagating wave? These are mechanisms for additional wave distortion (harmonics). Hysteresis and discrete memory provide a model where harmonics are generated from the nonlinear stress-strain curve and from the cusps of the hysteresis loop (discrete memory). The discussion of the theory has been covered elsewhere. For example, *Guyer et al.* [1995a, b] have included hysteresis and discrete memory in the nonlinear wave equation for propagating waves. However, the inclusion of hysteresis and discrete memory in the perturbation expansion is not sufficient as yet in providing us with the tools to directly calculate the nonlinear coefficients in our work. Our theoretical approach is under appropriate modification at present.

Our work shows further that because the classical perturbation theory may not be directly applied to rock, the information about the nonlinear response of a given rock sample is not necessarily obtained in a straightforward manner as it would be in a material that can be modeled applying classical nonlinear theory. Thus application of this method at present is perhaps best suited to comparative study of rocks.

Modulus and Excitation Versus Strain

The excitation-strain curve, for example, that shown in Figure 4 for Lavoux limestone, provides some measure of the modulus. This makes intuitive sense because as the excitation increases, energy is transferred into harmonics. The result of measuring the fundamental amplitude is that the calculated strain is smaller than predicted in the absence of energy transfer to harmonics, i.e., in the absence of elastic nonlinearity. The strain at the fundamental frequency is smaller than it should be for a given excitation. Thus the deviation from linearity in the excitation-strain curve is a measure of the energy transfer, in other words, the nonlinearity itself. We can be certain that the curve is not a source or instrumentation effect based on the elastically "linear" materials we have studied. Figure 2b shows such an example for polycarbonate. The excitation-strain curves could be used to calculate nonlinear moduli β and δ because excitation can be directly related to applied force; however, if hysteresis and discrete memory are active, then this would not be a useful exercise because the downgoing curve for excitation-strain would differ, and we are unable to measure the strain in this direction.

Lessons for Measurement of Q and Modulus

An important lesson from observation of peak shift is that Q cannot be reliably measured in this circumstance. The imaginary portion of the nonlinear modulus is the attenuation, and it is related in a very complex manner to the width of the peak and the associated harmonics [e.g., *McCall*, 1993; *Van Den Abeele*, 1996]. Therefore measurement of Q for anything but a perfectly linear (i.e., symmetric) resonant curve is not easily interpreted. In fact, even applying the results of an apparent linear resonance curve can be misleading. As our experience with chalk shows, it is possible to observe little or no resonant peak shift simultaneous with even enormous harmonic generation. The presence of harmonics will result in an underestimate of Q.

Sweep Rate and Relaxation Effects

We have not addressed sweep rate effects in this paper. We have examined rate dependence and have observed obvious rate dependent effects on the resonance curves. The resonance curves maintain the same general character if, for example, the sweep rate is increased. Our experiments were conducted at rates we deemed reasonable after numerous empirical tests. In addition, we have observed relaxation effects after a frequency sweep in some rocks. We have noted that it may take tens of seconds or up to several minutes for a rock to return to its original "linear" elastic state after a large-amplitude frequency sweep. In any case, these effects do not affect the conclusions presented here but must be accounted for in a complete theory.

Application of Nonlinear Elastic Measurements?

A fundamental question remains as to the value of measuring and understanding nonlinear elasticity in rock over and above academic interest. To first order, the nonlinear elastic response is certainly related to the microstructure and macrostructure of the material, the grain to grain contacts, the microcracks, joints, etc. The contained fluid also plays a very important role. The sensitivity of the nonlinear response to the structure and fluid content is far larger than that of standard linear measurements of wave speed, modulus, and attenuation. The problem is that these measurements are difficult to make and great care must be taken in separating the apparatus effects that can be identical. These are problems that are surmountable and the rewards may be great. We believe that the work presented in this paper and work on nonlinear elasticity by our group and other groups will lead us to a new level of

understanding the makeup of materials (new methods of quantifying the features that contribute to the nonlinear response in manners that were previously unrealized by application of linear methods).

Conclusions

We have illustrated the nonlinear response of rock by monitoring resonant peak shift and harmonic generation in several sedimentary rock types under a variety of saturation conditions. We compared results from numerous "linear" elastic standards such as PVC and Plexiglas to be certain that the observations resulted from the nonlinear response of the materials rather than the associated apparatus. General observations are difficult to make because the response of the different rocks is highly varied. There is no clear relation between peak shift and harmonic generation, for instance. Harmonics always accompany peak shift, but harmonics can exist with little or no resonant peak shift. As a result, great care must be taken when measuring and interpreting modulus and Q from resonance experiments. This is not a new result [e.g., *Winkler et al.*, 1979]; however, it is clear from our work that initiation of peak shift cannot be relied on for the onset of nonlinear elastic response. On the contrary, the only reliable method is to monitor harmonic generation. General observations that hold for all rocks over the dynamic strain intervals studied (up to 10^{-5} in the rocks and 10^{-4} in the standards) include the following. As in all nonlinear oscillators, the upward and downward frequency sweep is always different in the rocks studied, and the resonant frequency always shifts downward. Odd harmonics tend to dominate over even harmonics in amplitude. The excitation-strain curve is nearly always nonlinear in rocks and always linear in the standards. We have further demonstrated that the classical approach to modeling nonlinear oscillators does not hold for rocks. We believe the key difference between rocks and a classic nonlinear oscillator is the presence of discrete memory and hysteresis in rock.

The ramifications of monitoring nonlinear response in rock may ultimately effect many areas of research in geoscience including seismology, where the spectral distortion of seismic waves during propagation must be considered [e.g., *Johnson and McCall*, 1994; *Bulau et al.*, 1984; *Beresnev et al.*, 1995]. Other areas of research include rock mechanics and materials science where the nonlinear response of a material may be used for characterization purposes. In addition, characterization of material property change by monitoring nonlinear response may be of value. For instance, these changes include variations in water saturation for porous media, change in response to variations in stress, change induced by fatigue damage, etc.

Acknowledgments. This work was performed under the auspices of the Offices of Basic Energy Research, Engineering and Geoscience (contract W-7405-ENG-36), U.S. Department of Energy with the University of California, and the Institut Français du Pétrole. We thank Michel Masson for experimental assistance and Thomas Shankland and Albert Migliori for helpful discussions. We thank G. D. Meegan, who originally suggested conducting the experiments. We are deeply indebted to Katherine McCall, Koen Van Den Abeele, and Robert Guyer, who have contributed much to our understanding of the phenomena described here, and K. Van Den Abeele and James Ten Cate for critical review of the manuscript.

References

Bakulin V. N., and A. G. Protosenya, Nonlinear effects in travel of elastic waves through rocks, *Trans. USSR Acad. Sci., Earth Sci. Sect.*, *263*, 314–316, 1982.

Beresnev, I. A., and A. V. Nikolaev, Experimental investigations of nonlinear seismic effects, *Phys. Earth Planet. Inter.*, *50*, 83–87, 1988.

Beresnev, I. A., K.-L. Wen, and Y. T. Yeh, Seismological evidence for nonlinear elastic ground behavior during large earthquakes, *Soil Dyn. Earthquake Eng.*, *14*, 103–114, 1995.

Birch, F., Compressibility; elastic constants, in *Handbook of Physical Constants*, edited by S. P. Clark, Jr., pp. 97–174, Geol. Soc. of Am., Boulder, Colo., 1966.

Boitnott, G. N., Fundamental observations concerning hysteresis in the deformation of intact and jointed rock with applications to nonlinear attenuation in the near source region, in *Proceedings of the Numerical Modeling for Underground Nuclear Test Monitoring Symposium, Durango, CO., 1993*, edited by S. R. Taylor and J. R. Kamm, pp. 121–134, *Rep. LA-UR-93-3839*, Los Alamos Natl. Lab., Los Alamos, N. M., 1993.

Bonner, B. P., and B. J. Wanamaker, Acoustic nonlinearities produced by a single macroscopic fracture in granite, in *Review of Progress in Quantitative NDE*, vol. 10B, edited by D. O. Thompson and D. E. Chimenti, pp. 1861–1867, Plenum, New York, 1991.

Bulau, J. R., B. R. Tittmann, and M. Abdel-Gawad, Nonlinear wave propagation in rock, paper presented at the 1984 IEEE Ultrasonics Symposium, Inst. of Electr. and Electr. Eng., 1984.

Courant, R., and K. O. Friedrichs, *Supersonic Flow and Shock Waves*, Wiley-Interscience, New York, 1948.

Gist, G. A., Fluid effects on velocity and attenuation in sandstones, *J. Acoust. Soc. Am.*, *96*, 1158–1173, 1994.

Guyer, R. A., K. R. McCall, and G. N. Boitnott, Hysteresis, discrete memory and nonlinear wave propagation in rock, *Phys. Rev. Let.*, *74*, 3491–3494, 1995a.

Guyer, R. A., K. R. McCall, P. A. Johnson, P. N. J. Rasolofosaon, and B. Zinszner, Equation of state hysteresis and resonant bar measurements on rock, in *Proceedings of 35th U.S. Symposium on Rock Mechanics*, edited by J. J. K. Daemen and R. A. Schultz, pp. 177–181, A. A. Balkema, Rotterdam, 1995b.

Holcomb, D. J., Memory, relaxation, and microfracturing in dilatant rock, *J. Geophys. Res.*, *86*, 6235–6248, 1981.

Johnson, P. A., and K. R. McCall, Observation and implications of nonlinear elastic wave response in rock, *Geophys. Res. Lett.*, *21*, 165–168, 1994.

Johnson, P. A., and P. N. J. Rasolofosaon, Nonlinear elasticity and stress-induced anisotropy in rock, *J. Geophys. Res.*, *101*, 3113–3124, 1996.

Johnson, P. A., and T. J. Shankland, Nonlinear generation of elastic waves in granite and sandstone: Continuous wave and travel time observations, *J. Geophys. Res.*, *94*, 17,729–17,733, 1989.

Johnson, P. A., T. J. Shankland, R. J. O'Connell, and J. N. Albright, Nonlinear generation of elastic waves in crystalline rock, *J. Geophys. Res.*, *92*, 3597–3602, 1987.

Krech, W. W., F. A. Henderson, and K. E. Hjelmstad, A standard rock suite for rapid excavation research, *U.S. Bur. Mines, Rep. Invest. RI 7865*, 1974.

Landau, L. D., and E. M. Lifshitz, *Theory of Elasticity*, 3rd ed., Pergamon, Tarrytown, N. Y., 1986.

Liu, F., Nonlinear elasticity, seismic anisotropy and petrophysical properties of reservoir rocks, Ph.D. dissertation, Stanford Univ., Stanford, Calif., 1994.

Lucet, N., and B. Zinszner, Effects of heterogeneities and anisotropy on sonic and ultrasonic attenuation in rocks, *Geophysics*, *57*, 1018–1026, 1992.

McCall, K. R., Theoretical study of nonlinear acoustic wave propagation, *J. Geophys. Res.*, *99*, 2591–2600, 1993.

McCall, K. R., and R. A. Guyer, Equation of state and wave propagation in hysteretic nonlinear elastic material, *J. Geophys. Res.*, *99*, 23,887–23,897, 1994.

Meegan, G. D., P. A. Johnson, R. G. Guyer, and K. R. McCall, Observations of nonlinear elastic wave behavior in sandstone, *J. Acoust. Soc. Am.*, *94*, 3387–3391, 1993.

Murphy, W. F., III, Effects of microstructure and pore fluids of the acoustic properties of granular sedimentary materials, Ph.D. dissertation, Stanford Univ., Stanford, Calif., 1982.

Ostrovsky, L. A., Wave processes in media with strong acoustic nonlinearity, *J. Acoust. Soc. Am.*, *90*, 3332–3337, 1991.

Stoker, J. J., *Nonlinear Vibrations in Mechanical and Electrical Systems*, 81 pp., Wiley-Interscience, New York, 1950.

Van den Abeele, K. E.-A., Elastic pulsed wave propagation in media with second or higher order nonlinearity, 1, Theoretical framework, *J. Acoust. Soc. Am.*, in press, 1996.

Winkler, K., A. Nur, and M. Gladwin, Friction and seismic attenuation in rocks, *Nature*, *277*, 528–531, 1979.

Zinov'yeva, G. P., I. I. Nesterov, Y. L. Zdhakhin, E. E. Artma, and Y. V. Gorbunov, Investigation of rock deformation properties in terms of the nonlinear acoustic parameter, *Trans. USSR Acad. Sci. Earth, Earth Sci. Sect.*, *307*, 337–341, 1989.

P. A. Johnson, EES-4, MS D443, Los Alamos National Laboratory, Los Alamos, NM 87545. (e-mail: johnson@seismo5.lanl.gov)

P. N. J. Rasolofosaon and B. Zinszner, Institut Français du Pétrole, B. P. 311-92506, Rueil Malmaison Cedex, France. (e-mail: patrick.rasolofosaon@ifp.fr; bernard.zinszner@ifp.fr)

(Received July 24, 1995; revised February 12, 1996; accepted February 20, 1996.)